Koch, M., Wright, K. E., Otto, O., Herbig, M., Salinas, N. D., Tolia, N. H., Satchwell, T., Guck, J., Brooks, N. J., & Baum, J. (2017). Plasmodium falciparum erythrocyte-binding antigen 175 triggers a biophysical change in the red blood cell that facilitates invasion. *Proceedings of the National Academy of Sciences of the United States of America*, *114*(16), 4225-4230. https://doi.org/10.1073/pnas.1620843114

**Classification:** BIOLOGICAL SCIENCES (Microbiology) | PHYSICAL SCIENCES (Biophysics and Computational Biology)

# *Plasmodium falciparum* erythrocyte binding antigen-175 triggers a biophysical change in the red blood cell that facilitates invasion

Marion Koch[1], Katherine E. Wright[1], Oliver Otto[2], Maik Herbig[2], Nichole D. Salinas[3], Niraj H. Tolia[3], Timothy J. Satchwell[4], Jochen Guck[2], Nicholas J. Brooks[5]* and Jake Baum[1]*

[1] Department of Life Sciences, Imperial College London, London, UK.

[2] Biotechnology Center, Technische Universität Dresden, Dresden, Germany.

[3] Department of Molecular Microbiology and Microbial Pathogenesis, Washington University School of Medicine, Saint Louis, Missouri, USA.

[4] School of Biochemistry, Biomedical Sciences Building, University Walk, Bristol, UK.

[5] Department of Chemistry, Imperial College London, London, UK.

***Corresponding Authors:**

Dr Jake Baum. Department of Life Sciences, Imperial College London, Exhibition Road, South Kensington, London, SW7 2AZ, UK. Tel: +44 (0)207 5945420; Email: jake.baum@imperial.ac.uk

Dr Nicholas J. Brooks. Department of Chemistry, Imperial College London, Exhibition Road, South Kensington, London SW7 2AZ, UK. Tel: +44 (0)20 7594 2677; Email: n.brooks@imperial.ac.uk

**Keywords:** Erythrocyte; Merozoite; Malaria; Plasmodium; Real Time Deformability Cytometry; Flicker Microscopy.

## Abstract

Invasion of the red blood cell by the *Plasmodium* parasite defines the start of malaria disease pathogenesis. To date, experimental investigations into invasion have focused predominantly on the role of parasite adhesins or signaling pathways and the identity of binding receptors on the red cell surface. A potential role for signaling pathways within the erythrocyte, which might alter red cell biophysical properties to facilitate invasion, have largely been ignored. The parasite erythrocyte binding antigen (EBA)-175, a protein required for entry in most parasite strains, plays a key role by binding to glycophorin A (GPA) on the red cell surface, though the function of this binding interaction is unknown. Here using real-time deformability cytometry and flicker spectroscopy to define biophysical properties of the erythrocyte, we show that EBA-175 binding to GPA leads to an increase in the cytoskeletal tension of the red cell and a reduction in the bending modulus of the cell's membrane. We isolate the changes in the cytoskeleton and membrane and show that reduction in bending modulus is directly correlated with parasite invasion efficiency. These data strongly imply that the malaria parasite primes the erythrocyte surface through its binding antigens, altering the biophysical nature of the target cell, thus reducing a critical energy barrier to invasion. This would constitute a paradigm shift in our concept of malaria parasite invasion, suggesting it is in fact a balance between parasite and host cell physical forces working together to facilitate entry.

## Significance Statement

The blood-stage malaria parasite, the merozoite, invades the human red blood cell using receptor ligand interactions between parasite and host cell surface, yet the function of these interactions to invasion is not known. We have analysed the binding between one key merozoite invasion ligand, called EBA175, to glycophorin A on the red blood cell surface (the most dominant surface antigen) and explored how this affects the biophysical properties of the red cell. Using a combination of

imaging techniques, we demonstrate that the malaria parasite changes the biophysical nature of the red cell, facilitating its own entry by effectively reducing the energy barrier to invasion. This is the first demonstration of a red cell biophysical contribution to merozoite entry.

\body

## Introduction

Malaria infections cause approximately 438,000 deaths per year – most of which are due to the protozoan parasite *Plasmodium falciparum* (1). While extensive eradication efforts have helped to reduce the incidence of malaria, the spread of drug resistance is a growing concern and novel treatments are urgently needed (2). Throughout the *Plasmodium* lifecycle, parasites shuttle between replicative and motile lifecycle stages, with the motile forms or *zoites* highly adapted to the invasion of host cells. During the blood stages of infection, the merozoite targets and invades the red blood cell (RBC) rapidly (<30s), in a process that involves numerous parasite ligands and host cell receptors (3). Merozoite entry is a multi-step process commencing with initial attachment and ending with parasite actomyosin driven invasion (4). Although extensive cellular and molecular detail of each step has been elucidated (5, 6), there is still little mechanistic understanding of the role of each protein involved or the signalling events within the erythrocyte that accompany entry (7).

Initial attachment to the RBC surface is likely mediated by merozoite surface proteins (MSPs). Subsequently, the key signalling and strong attachment interactions between host and parasite membranes are thought to be mediated by two major classes of adhesins, released either before or concomitantly with invasion at the merozoite apex. These adhesins are the erythrocyte binding-like (EBL, or erythrocyte binding antigens, EBA) and reticulocyte binding-like (RBL or Rh) protein families, comprised in *P. falciparum* of the EBA175, EBA140, EBA181 and EBL1 and Rh1, Rh2a, Rh2b, Rh4 and Rh5 proteins, respectively (8, 9). Although the binding between Rh5 and its receptor Basigin is the only ligand-receptor interaction identified to date that is essential for all *P. falciparum* strains (10), EBA175 and its interaction with Glycophorin A (GPA) is nonetheless functionally almost universally important (11). When EBA175 function is ablated (e.g. genetically), some strains are able to switch to an alternative invasion pathway utilising the interaction of Rh4 and its receptor CR1 (12). The precise function of each ligand-receptor complex during invasion is largely unknown, however, in recent years it has become clearer that these interactions do not

merely serve for adhesion, but instead may be involved in transducing signals into either the merozoite (13, 14) or potentially the RBC(7).

Recently we attempted to model invasion in terms of the biophysical forces required to enwrap a merozoite towards full RBC entry; of particular focus were properties of membrane tension (which, in the RBC, is primarily provided by the cytoskeleton) and bending modulus (the energy required to cause bending of the lipid bilayer) (15). Whilst the actin-myosin motor provides a critical force to push the merozoite into the host cell, other factors could significantly contribute to lowering the energy barrier for invasion. These include energy gains from tight adhesion to the host cell (via receptor-ligand interactions) or manipulation of the host cell cytoskeletal or membrane properties, each of which could facilitate wrapping of the merozoite. Beyond malaria invasion biology, binding of two critical red cell receptors utilised by the merozoite during invasion (CR1 and GPA) have been shown to transmit biophysical changes to the RBC when bound by certain ligands (16, 17). To date, it has not been assessed whether parasite ligands during invasion transmit similar changes, and whether these influence invasion efficiency.

Here we have attempted to explore the hypothesis that parasite ligands prime the RBC by changing its biophysical properties, reducing the energy barriers for invasion. We demonstrate using two separate techniques that binding of the merozoite ligand EBA175 to its receptor GPA causes distinct biophysical changes to the RBC. EBA175 binding causes an increase in cytoskeletal tension, which is dependent on the cytoplasmic tail of the GPA protein. EBA175 binding also causes a reduction in the bending modulus of the membrane. Chemically induced reduction of the bending modulus significantly increases invasion efficiency, supporting our hypothesis that parasite-dependent RBC changes reduce the energy barrier for successful malaria parasite entry into the human erythrocyte.

## Results

### EBA175 region II binding to GPA alters RBC deformability

Theoretical models and phospho-proteomic studies suggest that the *Plasmodium falciparum* merozoite triggers host changes to facilitate its invasion on binding to the RBC (7, 15). To explore

whether this is mediated by erythrocyte binding antigens (EBA), we explored EBA175 binding to its RBC receptor GPA on overall erythrocyte biophysical properties. This receptor ligand interaction is specific; mediated by glycosylated residues on GPA which are absent in other glycophorin molecules (18). Utilising a recombinantly expressed receptor-binding region (region II) of EBA175 (rEBA175-RII) (19, 20) we first validated receptor specificity of the protein incubated with untreated or neuraminidase (Neu) treated human RBCs (Figure 1A), the latter ablating sialic acid residues on GPA, known to be crucial for binding (21).

Having demonstrated the Neu binding-specificity of the rEBA175-RII ligand, we next incubated RBCs with different concentrations of the protein before analysing cells using real-time deformability cytometry (RT-DC) (22). This flow cytometry-based technique permits the label-free analysis of approximately 1,000 cells/sec, making it particularly useful for analysing cells that show natural variability in their biophysical characteristics such as RBCs (23). For untreated cells, analysis of deformation versus cell size (cross-sectional area) found that most cells were contained within one population with an average cross-sectional area of 36.5 $\mu m^2$(Figure 1B). A second population of larger cells (>50 $\mu m^2$), when manually inspected, was found to contain cell clumps, predominantly doublets (Figure 1B). Since RT-DC analysis is based on extracting cell contours to quantify cell deformation, and contours of doublets could potentially lead to a skew in the data dependent on the shape of the cell clump, such clumps were removed from downstream analyses by creating a gate containing the singlet RBC population (Figure 1B). Incubation of RBCs with rEBA175-RII resulted in many of the cells forming larger clumps (Figure 1C). These aggregates were removed from our analysis as described above. RT-DC measurements of RBCs treated with 25-50µg/ml rEBA175-RII, a concentration similar to that previously used for antibody studies (24), revealed a significant reduction in RBC deformability (Figure 1D). At higher concentrations of rEBA175-RII, a significant proportion of RBCs were present in cell doublets or clumps complicating analysis using this technique. To test the specificity of these identified biophysical changes, rEBA175-RII was also incubated with Neu-treated RBCs (Figure 1E). These cells do not show a decrease in deformability, confirming this effect to be rEBA175-RII binding specific.

**Flicker Spectroscopy of RBC biophysical parameters**

To determine the cause of biophysical changes seen by real-time deformability cytometry, we sought to employ a method that would permit independent measurement of the tension and bending modulus of the RBC surface on EBA175 binding. Membrane fluctuation analysis (flicker spectroscopy) has been used extensively as a method for mechanical characterization of vesicles (25, 26) and erythrocytes (27-29) at the single cell level. Critically for our purposes, the cytoskeletal and lipid membrane properties dominate different ranges of the fluctuation spectrum. It is well established that tension in RBCs largely arises from the cytoskeleton underlying the erythrocyte bilayer and changes in tension are primarily reflected in the lower fluctuation mode numbers (SI Appendix Figure S1). Conversely, variations in the RBC bending modulus are largely expected to come from changes to the cell membrane and this is reflected in the higher mode numbers (Figure S1) (27).

While many chemicals, known to induce cellular biophysical changes, have wide-ranging effects causing both cytoskeletal and membrane alterations, we sought to validate the assumptions outlined above by inducing several controlled biophysical changes in RBCs to confirm the reliability of flicker spectroscopy in detecting erythrocyte cytoskeletal and membrane changes. Glutaraldehyde preferentially crosslinks proteins and is therefore expected to affect cytoskeletal properties (i.e. tension), though it can interact with and crosslink amino groups on phospholipids (30). In agreement with this, at 0.01% glutaraldehyde, RBC tension increased significantly (Figure 2A) with no significant effect on bending modulus (Figure 2B). Figure S2A shows representative spectra of individual RBCs from each treatment sample. At higher concentrations, membrane oscillations were reduced to negligible levels (Figure S2A), suggesting that all protein and membrane constituents had been completely crosslinked. As a further test, we explored diamide, an oxidising reagent that has previously been shown to cause tightening of the RBC cytoskeleton and reduce RBC deformability (31) (Figure 2C-D, S2B). Treatment of RBCs with 50 and 500 μM diamide resulted in a concentration dependent increase in tension (Figure 2C) in line with previously published work (31). While the exact effect of RBC treatment with diamide on its bending modulus has not previously been tested, the bending modulus change (Figure 2D) is

comparable to other oxidative reagents, which have been shown to cause lipid peroxidation resulting in higher bending modulus (32) as well as reduced membrane fluidity (33).

We next sought to isolate the effect of changing bending modulus, specifically targeting RBC lipid properties. X-Ray diffraction measurements and molecular dynamic simulations suggest that DMSO disrupts interactions between the headgroups of different lipids, decreasing bilayer thickness and increasing membrane fluidity (34, 35). These simulations suggest that at a DMSO concentration of 5% the average area between the inner and outer membrane layer would be reduced by ~10%. Similarly, at 15% DMSO the area reduction would be expected to be >55%. Tests at both concentrations by flicker spectroscopy (Figure 2E-F, S2C) demonstrated that the bending modulus was indeed reduced at both 5% and 15% DMSO (Figure 2F); however, this was only statistically significant at 15%. Of note, at this concentration some RBCs (omitted from analysis) undergo morphological changes wherein tension (Figure 2E) is also affected, likely due to the stress caused by the high percentage of DMSO used.

As a final way of experimentally validating our flicker approach, we investigated use of 7-ketocholesterol (7KC), a probe that reduces lipid packing and lipid order by integrating into the RBC membrane (36). We found that 7KC significantly and specifically reduces bending modulus without affecting tension properties (Figure 2G-H, S2D). Collectively, these data demonstrate our ability to decouple membrane and cytoskeletal changes in the RBC using flicker spectroscopy.

**EBA175 binding to GPA triggers specific RBC cytoskeletal and membrane changes**

Having established adequate controls, we next investigated how EBA175 binding to the RBC affects cytoskeletal and membrane properties of the target cell. In agreement with the RT-DC data as well as previous biophysical data examining GPA binding by antibody moieties (24), we found a clear concentration-dependent increase in RBC tension on addition of rEBA175-RII (Figure 3A, S3A). At very low concentrations, we noticed a small but reproducible reduction in tension at low rEBA175-RII concentrations suggesting the RBC biophysical response to rEBA175-RII might be a non-linear concentration dependent effect at low concentrations (Figure 3A). Noticeably, this was also present using RBCs pre-treated with neuraminidase supporting the notion that a small number

of binding sites are still present following enzyme treatment, giving rise to the small effect alone. For bending modulus, rEBA175-RII binding significantly reduced values across a wide range of concentrations (Figure 3B, S3B). This was dependent on sialic acid residues, confirming that the change is binding-specific (Figure 3B). The effects of rEBA175-RII on RBC biophysical properties was reproducible across different RBC samples (Figure 3C-D, S3B).

**Significance of RBC tension for parasite invasion**

To investigate the relevance of the rEBA175-RII mediated tension and bending modulus changes to parasite invasion, each component was isolated to test their importance independently. Previous studies using anti-GPA antibodies have shown that the binding-mediated decrease in deformability occurs through signalling involving the GPA cytoplasmic tail (24). We therefore hypothesised that in the absence of this region, rEBA175-RII would not initiate an increase in tension. To test this hypothesis, we used RBCs isolated from an individual with an extremely rare human glycophorin variant, the Miltenberger class V (MiV) condition, in which GPA and GPB is replaced with a hybrid GPA-GPB protein. This protein contains the extracellular regions of GPA, but the shortened intracellular tail of GPB (18, 37), which is not predicted to interact with the underlying cytoskeleton as wild-type GPA does. Entirely in line with predictions, rEBA175-RII did not cause an increase in tension in MiV RBCs (Figure 4A, S4). Indeed, in the absence of the cytoplasmic GPA tail, EBA175 binding caused instead a small but noticeable decrease in tension. Unexpectedly, the bending modulus decrease still occurred in MiV cells (Figure 4B, S4). Since changes in membrane organisation still occur in the absence of the GPA cytoplasmic tail, this suggests that biophysical change is independent of the interaction between the cytoplasmic tail of GPA and the RBC interior. While the importance of the glycophorins for erythrocyte invasion by *P. falciparum* is indisputable (12, 18, 38), some parasite strains have evolved to invade independently of GPA. If the GPA tail-mediated tension change following EBA175 binding was required for invasion, parasites that relied on GPA for invasion would be expected to invade MiV RBCs less efficiently than parasites invading via a GPA-independent pathway. To test this, we purified mature schizonts from two strains, W2mefΔRh4 and W2mefΔEBA175, and incubated these with either MiV cells or normal RBCs. W2mefΔRh4 parasites, lacking Rh4, rely on the EBA175-GPA interaction for invasion (12).

W2mefΔEBA175 are, in contrast, able to invade RBCs independently of EBA175-GPA. No significant differences were found in the ability of either parasite strain to invade MiV RBCs (Figure 4C). This suggests that, contrary to expectations, the tension increase triggered by the cytoskeletal tail of GPA is not required for invasion.

**Significance of RBC bending modulus for parasite invasion**

Having assessed the role of tension in invasion, we next sought to directly assess the relationship between bending modulus and *P. falciparum* invasion. Since bending modulus describes the amount of energy required to bend a lipid bilayer, a reduction in this property would also decrease the energy barrier to invasion and would be, as such, predicted to increase parasite invasion efficiency (15). This might derive from changes in lipid composition, e.g. the percentage of cholesterol (39), asymmetry between inner and outer membrane leaflets (25) or the extent of lipid chain saturation or modification (40), each of which have been described to affect membrane thickness and bending modulus. To begin to assess whether the decrease in bending modulus following GPA binding resulted from changes in membrane asymmetry, we tested whether binding of rEBA175-RII to its RBC receptor triggered calcium changes (associated with scramblase activation in the RBC) or externalisation of lipid moieties normally limited to the internal membrane leaflet. Fluo-4AM and Annexin V labelling of RBCs in the presence or absence of rEBA175-RII found no evidence for calcium signalling (marked by Fluo-4AM) (Figure 5A) or for a differential externalization of phosphatidylserine (marked by Annexin V) (Figure 5B), as opposed to incubation with the calcium channel activator Yoda 1 (used here as a positive control) (41). This suggests asymmetry is not the direct cause of the reduction in bending modulus. At present, therefore, the direct cause of the reduction in bending modulus remains to be elucidated.

To explore the significance of a reduction in bending modulus, and given the essential role of the GPA invasion route for sialic-acid dependent invasion, which is not attributable to the changes in tension, we investigated whether experimentally induced reduction in this parameter improved invasion efficiency. 7KC has been shown to reduce lipid packing/order in membranes (42) and as demonstrated above (Figure 2G-H, S2D) leads to a reduction in bending modulus. Pre-treatment

of RBCs with 7KC would therefore be predicted to increase invasion efficiency if parasite-induced reduction of bending modulus is a key parameter for invasion. RBCs pre-treated with 7KC to decrease the bending modulus were more readily invaded by *P. falciparum* merozoites (Figure 5C-D). These results demonstrate a clear linkage between parasite-induced changes in the RBC surface and invasion ligand binding, the direct consequence of which is to change RBC biophysical properties to increase invasion efficiency. Combined, these data strongly imply that *P. falciparum* merozoites alter the target erythrocyte's biophysical properties prior to invasion to facilitate their own entry.

## Discussion

Here, complementary biophysical approaches demonstrate that binding of the malaria parasite invasion ligand EBA175 to its host cell receptor GPA triggers a biophysical response in the RBC. Exploration of this change identified a reduction in the RBC bending modulus on binding, which itself significantly increases invasion efficiency. Thus, consistent with biophysical predictions of the energetics involved in invasion (15), the malaria parasite does appear to alter the RBC surface to facilitate its own entry.

One of the key challenges with biophysical approaches that explore changes in RBC properties is differentiating between contributions arising from cytoskeletal or membrane changes. By using a number of chemical reagents, previously described to affect cytoskeletal and lipid properties (i.e. glutaraldehyde, diamide, DMSO and 7-ketocholesterol), we confirm that we can distinguish between changes occurring within the cytoskeletal and lipid membrane components described by tension and bending modulus. This provides a key foundation for investigating the RBC biophysical response to binding by the invasion ligand EBA175.

Both biophysical techniques used in this study identified an increased rigidification (reduction in RBC deformability/increase in tension) at the higher concentrations tested (≥10 ug/ml rEBA175-RII) which is in agreement with previous work using GPA-antibodies (24, 43, 44). Of interest, we measured a small, but repeatable, reduction in tension at low concentrations by flicker spectroscopy. This would suggest that the interaction between EBA175 and GPA, and resulting changes in the RBC, is not a linear relationship. In the context of merozoite invasion, where the

absolute number of EBA175 molecules at the RBC interface is unknown, several different scenarios could arise that impact on the invasion process. At the invasion site, a higher local EBA175 concentration could significantly change the local tension and bending modulus conducive to invasion (see model, SI Appendix Figure S5). Additionally, diffuse EBA175 on the RBC surface (or shed from the parasite surface (45)) may affect the wider RBC, either triggering further changes conducive to invasion, or potentially binding to bystander RBCs thereby lowering their energy barrier for invasion events.

Of the two key changes in tension and bending modulus, the cytoskeletal changes, as mediated by the cytoplasmic tail of GPA, surprisingly were not found to be essential for invasion *in vitro*. This contradicted our expectation that increased crosslinking of the GPA tail upon EBA175 binding might be functional for invasion, for instance serving as a focal point where the RBC cytoskeleton could be opened up around the invading parasite or providing stability for the tight junction (46). This suggests that direct crosslinking of GPA to the cytoskeleton via its cytoplasmic tail does not significantly impact invasion efficiency.

In contrast, a reduction in bending modulus, which still occurred in MiV cells, appears to be one of the critical roles of EBA175 binding. Bending modulus is an intrinsic property of the lipid bilayer that describes the amount of energy required to bend it and is affected by lipid composition, membrane thickness and membrane asymmetry. These properties regulate numerous cellular functions through membrane curvature(47), endocytosis(48), opening of protein channels(49), and initiation of signalling processes(50), and unsurprisingly are often exploited by intracellular pathogens(40, 51). We were therefore intrigued by the possibility that the architecture of the lipid bilayer might be exploited by the merozoite during invasion. Invasion into RBCs pre-treated with 7KC, mimicking the bending modulus decrease caused by GPA binding, demonstrated that invasion efficiency for both sialic acid-dependent (W2mefΔRh4) and -independent (W2mefΔEBA175) strains significantly increased. This strongly suggests that parasite-host interactions trigger RBC biophysical responses that contribute to invasion efficiency. What is the nature of this change? Since the decrease in bending modulus is not dependent on the cytoplasmic tail of GPA, this change might arise through a reduction in the lateral pressure within

the membrane caused by a conformational change in GPA. Just as transmembrane proteins (i.e. mechanosensors) can be regulated by forces exerted on them by the lipid bilayer, transmembrane and membrane-associated proteins are also capable of affecting membrane properties by modulating the bilayer structure (52). Dimerization of EBA175 around GPA could lead to a conformational change in GPA within the membrane, effectively freeing up space in the bilayer, reducing lateral pressure and hence bending modulus (25). That EBA175 binding causes a signalling cascade in the RBC is not surprising, given the strong RBC deformations that occur during invasion are dependent on the EBA175-GPA interactions (6, 13). Future efforts should focus on identifying molecular and/or signalling events that lead to these biophysical changes.

## Materials and Methods

Methods for parasite culture, measuring invasion efficiency, erythrocyte binding and flow cytometry followed standard approaches. For full description of these, and details of statistical analysis, please see SI Appendix.

### Real Time Deformability Cytometry (RT-DC)

50 µl packed RBCs were incubated with appropriate concentrations of EBA175-RII at room temperature for 1 hour before being drawn into a 1ml syringe, and connected to a custom-made Polydimethylsiloxane (PDMS) microfluidic chip. Cells were recorded at approximately 2,000 fps using a CMOS camera (MC1362, Mikrotron, Germany) and a NI-1433 Frame Grabber (National Instruments) as they travel through the PDMS chip at flow rates of 0.4 – 0.12 µl/sec. The extent of deformation is extracted from the cross-sectional area calculated using a custom derived contour tracking algorithm. For full discussion of the technique and analysis see (22).

### Flicker Spectroscopy

RBCs were diluted into RPMI-1640 (Sigma-Aldrich) at 0.5% haematocrit and incubated at room temperature for 30 minutes. Fluctuation videos were recorded on a Nikon Ti Microscope (objective lens: Nikon Plan Apo 100x 1.4 NA oil immersion) using an OrcaFlash4.0 CMOS camera. Approximately 4,500 frames were recorded at a frame rate of 150 fps and exposure time of 1 ms. Data analysis was carried out using a custom-built LabVIEW (National Instruments) program which

detects and extracts membrane contours from each frame with subpixel resolution. Full details of membrane fluctuation analysis is given elsewhere (27). Briefly, the deviation of each contour from the mean membrane position was decomposed into fluctuation modes by Fourier transforming to give a fluctuation power spectrum of mean square mode amplitudes at the cell equator ($h^2$ ($q_x$, y = 0)) as a function of mode wavenumber ($q_x$). From this data, the bending modulus ($\kappa$) and tension ($\sigma$) can be fitted using the following equation:

$$\langle h(q_x, y=0)^2 \rangle = \frac{1}{L}\frac{k_B T}{2\sigma}\left(\frac{1}{q_x} - \frac{1}{\sqrt{\frac{\sigma}{k_c} + {q_x}^2}}\right)$$

where $k_B$ is the Boltzmann constant, T is temperature, and L is mean circumference of the cell contour. This model assumes that the cell surface behaves as a flat sheet and that we image the equator of the cell. When fitting the fluctuation data, mode numbers 4 and below were excluded due to significant influence of the cell shape (breakdown of the flat sheet assumption) and mode numbers beyond 20 were removed since these fluctuations lie outside the spatial and temporal resolution of the experiment. The tension and bending modulus terms dominate different parts of the fluctuation power spectrum (and can be attributed to distinct cellular properties as described below) and so can be independently resolved using a double parameter non-linear fit to the model above.

**Acknowledgments**

We thank P. Cicuta and A. Dufour for help in development of flicker analysis and S. Girardo for help with PDMS chips preparation. We acknowledge A. Cowman for generous provision of mutant *P. falciparum* W2m strains and N. Thornton for provision of Miltenberger V RBCs. The research was directly supported by the Wellcome Trust (Investigator Award 100993/Z/13/Z J.B.). We acknowledge Alexander von Humboldt Stiftung (Alexander von Humboldt Professorship to J.G.) and a TG70 research grant from the SMWK (O.O. and J.G.). T.J.S. is funded by the National Institute for Health Research Blood and Transplant Research Unit at the University of Bristol in partnership with NHS Blood and Transplant. M.K. is supported by a PhD scholarship from the UK Medical Research Council (MR/K501281/1). K.E.W. is supported through a Henry Wellcome

Postdoctoral Fellowship (107366/Z/15/Z). N.J.B. is supported by EPSRC programme grant EP/J017566/1.

## Authorship Contributions

M.K., K.E.W., N.J.B., and J.B. designed all experiments with contribution from T.J.S. for MiV work; M.K. and K.E.W. performed experiments; M.H and O.O. performed RT-DC experiments. N. D. S. and N.H.T. prepared purified recombinant protein. All authors contributed to manuscript preparation; M.K. and J.B. wrote the manuscript.

## Conflict of Interest Disclosures

O.O. is a co-founder of a company commercializing RT-DC. All other authors declare no competing financial interests.

## References

1. WHO (2016) World Malaria Report. (WHO).
2. Ashley EA*, et al.* (2014) Spread of artemisinin resistance in Plasmodium falciparum malaria. *N Engl J Med* 371(5):411-423.
3. Cowman AF, Berry D, & Baum J (2012) The cellular and molecular basis for malaria parasite invasion of the human red blood cell. *J Cell Biol* 198(6):961-971.
4. Bargieri D*, et al.* (2014) Host cell invasion by apicomplexan parasites: the junction conundrum. *PLoS Pathog* 10(9):e1004273.
5. Riglar DT*, et al.* (2011) Super-Resolution Dissection of Coordinated Events during Malaria Parasite Invasion of the Human Erythrocyte. *Cell Host Microbe* 9(1):9-20.
6. Weiss GE*, et al.* (2015) Revealing the sequence and resulting cellular morphology of receptor-ligand interactions during Plasmodium falciparum invasion of erythrocytes. *PLoS Pathog* 11(2):e1004670.
7. Zuccala ES*, et al.* (2016) Quantitative phospho-proteomics reveals the Plasmodium merozoite triggers pre-invasion host kinase modification of the red cell cytoskeleton. *Sci Rep* 6:19766.
8. Tham WH, Healer J, & Cowman AF (2012) Erythrocyte and reticulocyte binding-like proteins of Plasmodium falciparum. *Trends Parasitol* 28(1):23-30.
9. Paul AS, Egan ES, & Duraisingh MT (2015) Host-parasite interactions that guide red blood cell invasion by malaria parasites. *Curr Opin Hematol* 22(3):220-226.
10. Crosnier C*, et al.* (2011) Basigin is a receptor essential for erythrocyte invasion by Plasmodium falciparum. *Nature* 480(7378):534-537.

11. Duraisingh MT, Maier AG, Triglia T, & Cowman AF (2003) Erythrocyte-binding antigen 175 mediates invasion in Plasmodium falciparum utilizing sialic acid-dependent and -independent pathways. *Proc Natl Acad Sci U S A* 100(8):4796-4801.
12. Stubbs J*, et al.* (2005) Molecular mechanism for switching of P. falciparum invasion pathways into human erythrocytes. *Science* 309(5739):1384-1387.
13. Tham WH*, et al.* (2015) Plasmodium falciparum Adhesins Play an Essential Role in Signalling and Activation of Invasion into Human Erythrocytes. *PLoS Pathog* 11(12):e1005343.
14. Prinz B*, et al.* (2016) Hierarchical phosphorylation of apical membrane antigen 1 is required for efficient red blood cell invasion by malaria parasites. *Sci Rep* 6:34479.
15. Dasgupta S*, et al.* (2014) Membrane-wrapping contributions to malaria parasite invasion of the human erythrocyte. *Biophys J* 107(1):43-54.
16. Khoory J*, et al.* (2016) Ligation of Glycophorin A Generates Reactive Oxygen Species Leading to Decreased Red Blood Cell Function. *PLoS One* 11(1):e0141206.
17. Karnchanaphanurach P*, et al.* (2009) C3b deposition on human erythrocytes induces the formation of a membrane skeleton–linked protein complex. *J Clin Invest* 119(4):788-801.
18. Salinas ND, Paing MM, & Tolia NH (2014) Critical glycosylated residues in exon three of erythrocyte glycophorin A engage Plasmodium falciparum EBA-175 and define receptor specificity. *MBio* 5(5):e01606-01614.
19. Chen E, Paing MM, Salinas N, Sim BK, & Tolia NH (2013) Structural and functional basis for inhibition of erythrocyte invasion by antibodies that target Plasmodium falciparum EBA-175. *PLoS Pathog* 9(5):e1003390.
20. Salinas ND & Tolia NH (2014) A quantitative assay for binding and inhibition of Plasmodium falciparum Erythrocyte Binding Antigen 175 reveals high affinity binding depends on both DBL domains. *Protein Expr Purif* 95:188-194.
21. Sim BK, Chitnis CE, Wasniowska K, Hadley TJ, & Miller LH (1994) Receptor and ligand domains for invasion of erythrocytes by Plasmodium falciparum. *Science* 264(5167):1941-1944.
22. Otto O*, et al.* (2015) Real-time deformability cytometry: on-the-fly cell mechanical phenotyping. *Nat Methods* 12(3):199-202, 194 p following 202.
23. Costa M, Ghiran I, Peng CK, Nicholson-Weller A, & Goldberger AL (2008) Complex dynamics of human red blood cell flickering: alterations with in vivo aging. *Phys Rev E Stat Nonlin Soft Matter Phys* 78(2 Pt 1):020901.
24. Chasis JA, Reid ME, Jensen RH, & Mohandas N (1988) Signal transduction by glycophorin A: role of extracellular and cytoplasmic domains in a modulatable process. *J Cell Biol* 107(4):1351-1357.
25. Elani Y*, et al.* (2015) Measurements of the effect of membrane asymmetry on the mechanical properties of lipid bilayers. *Chem Commun (Camb)* 51(32):6976-6979.
26. Karamdad K, Law RV, Seddon JM, Brooks NJ, & Ces O (2016) Studying the effects of asymmetry on the bending rigidity of lipid membranes formed by microfluidics. *Chem Commun (Camb)* 52(30):5277-5280.
27. Yoon YZ*, et al.* (2009) Flickering analysis of erythrocyte mechanical properties: dependence on oxygenation level, cell shape, and hydration level. *Biophys J* 97(6):1606-1615.
28. Bokori-Brown M*, et al.* (2016) Red Blood Cell Susceptibility to Pneumolysin: CORRELATION WITH MEMBRANE BIOCHEMICAL AND PHYSICAL PROPERTIES. *J Biol Chem* 291(19):10210-10227.
29. Betz T, Lenz M, Joanny J-F, & Sykes C (2009) ATP-dependent mechanics of red blood cells. *Proc Natl Acad Sci USA* 106(36):15320-15325.
30. Hayat MA (1986) *Basic techniques for transmission electron microscopy*.
31. Sinha A, Chu TT, Dao M, & Chandramohanadas R (2015) Single-cell evaluation of red blood cell bio-mechanical and nano-structural alterations upon chemically induced oxidative stress. *Sci Rep* 5:9768.
32. Hale JP, Winlove CP, & Petrov PG (2011) Effect of hydroperoxides on red blood cell membrane mechanical properties. *Biophys J* 101(8):1921-1929.
33. Dobretsov GE, Borschevskaya TA, Petrov VA, & Vladimirov YA (1977) The increase of phospholipid bilayer rigidity after lipid peroxidation. *FEBS Lett* 84(1):125-128.

34. Notman R, Noro M, O'Malley B, & Anwar J (2006) Molecular basis for dimethylsulfoxide (DMSO) action on lipid membranes. *J Am Chem Soc* 128(43):13982-13983.
35. Gurtovenko AA & Anwar J (2007) Modulating the structure and properties of cell membranes: the molecular mechanism of action of dimethyl sulfoxide. *J Phys Chem B* 111(35):10453-10460.
36. Owen DM, Williamson DJ, Magenau A, & Gaus K (2012) Sub-resolution lipid domains exist in the plasma membrane and regulate protein diffusion and distribution. *Nat Commun* 3:1256.
37. Vignal A*, et al.* (1989) Molecular analysis of glycophorin A and B gene structure and expression in homozygous Miltenberger class V (Mi. V) human erythrocytes. *Eur J Biochem* 184(2):337-344.
38. Malaria Genomic Epidemiology N, Band G, Rockett KA, Spencer CC, & Kwiatkowski DP (2015) A novel locus of resistance to severe malaria in a region of ancient balancing selection. *Nature* 526(7572):253-257.
39. de Meyer FJ, Benjamini A, Rodgers JM, Misteli Y, & Smit B (2010) Molecular simulation of the DMPC-cholesterol phase diagram. *J Phys Chem B* 114(32):10451-10461.
40. Romer W*, et al.* (2007) Shiga toxin induces tubular membrane invaginations for its uptake into cells. *Nature* 450(7170):670-675.
41. Syeda R*, et al.* (2015) Chemical activation of the mechanotransduction channel Piezo1. *eLife* 4.
42. Rentero C*, et al.* (2008) Functional implications of plasma membrane condensation for T cell activation. *PLoS One* 3(5):e2262.
43. Chasis JA, Mohandas N, & Shohet SB (1985) Erythrocyte membrane rigidity induced by glycophorin A-ligand interaction. Evidence for a ligand-induced association between glycophorin A and skeletal proteins. *J Clin Invest* 75(6):1919-1926.
44. Knowles DW, Chasis JA, Evans EA, & Mohandas N (1994) Cooperative action between band 3 and glycophorin A in human erythrocytes: immobilization of band 3 induced by antibodies to glycophorin A. *Biophys J* 66(5):1726-1732.
45. O'Donnell RA*, et al.* (2006) Intramembrane proteolysis mediates shedding of a key adhesin during erythrocyte invasion by the malaria parasite. *J Cell Biol* 174(7):1023-1033.
46. Koch M & Baum J (2016) The mechanics of malaria parasite invasion of the human erythrocyte - towards a reassessment of the host cell contribution. *Cell Microbiol* 18(3):319-329.
47. Graham TR & Kozlov MM (2010) Interplay of proteins and lipids in generating membrane curvature. *Curr Opin Cell Biol* 22(4):430-436.
48. Pomorski T*, et al.* (2003) Drs2p-related P-type ATPases Dnf1p and Dnf2p are required for phospholipid translocation across the yeast plasma membrane and serve a role in endocytosis. *Mol Biol Cell* 14(3):1240-1254.
49. Charalambous K*, et al.* (2012) Engineering de novo membrane-mediated protein-protein communication networks. *J Am Chem Soc* 134(13):5746-5749.
50. Gaus K, Chklovskaia E, Fazekas de St Groth B, Jessup W, & Harder T (2005) Condensation of the plasma membrane at the site of T lymphocyte activation. *J Cell Biol* 171(1):121-131.
51. Ewers H*, et al.* (2010) GM1 structure determines SV40-induced membrane invagination and infection. *Nat Cell Biol* 12(1):11-18; sup pp 11-12.
52. Zimmerberg J & Kozlov MM (2006) How proteins produce cellular membrane curvature. *Nat Rev Mol Cell Biol* 7(1):9-19.

**Figure Legends**

**Figure 1.** rEBA175-RII mediated RBC biophysical changes. (A) Erythrocyte binding assay with rEBA175-RII (labelled as RII). Untreated human RBCs and neuraminidase (Neu) treated RBCs were incubated with rEBA175-RII. Bound protein was eluted with NaCl and presence of rEBA175-

RII evaluated by western blot. (B) Scatter plot of deformation versus cross-sectional area of control RBCs. Secondary populations of “larger cells” contains cell doublets or clumps. (C) rEBA175-RII treated RBCs caused a much higher percentage of cells to clump. These cells were removed from analysis from all samples. RBCs from three different donors were exposed to a range of rEBA175-RII concentrations (D) and show a concentration dependent reduction in RBC deformation. (E) Deformation of RBCs pre-treated with neuraminidase (Neu) was not significantly affected by treatment with rEBA175-RII. P-values comparing the treatment versus control, calculated using Linear Mixed Models (ns: non-significant, ** p<0.05, ** p<0.01, *** p<0.001, **** p<0.0001).*

**Figure 2.** Chemically-induced tension and bending modulus changes in RBCs measured by flicker spectroscopy. Summary of tension (σ) and bending modulus (κ) values of RBCs treated with Glutaraldehyde, (A-B), Diamide, (C-D), DMSO (E-F) and 7-KC (G-H). Each circle represents data from a single cell, solid line represents the median. Mean square amplitude ($h\ (q_x)^2\ (m)^2$) of contour fluctuation modes versus wave vector ($q_x$) of representative RBCs are shown in SI Figure S2. P-values comparing the treatment versus control, calculated using Mann-Whitney test (ns: non-significant, ** p<0.05, ** p<0.01, *** p<0.001, **** p<0.0001).*

**Figure 3.** rEBA175-RII mediated tension and bending modulus changes measured by flicker spectroscopy. (A-D) Summary of tension (σ) and bending modulus (κ) values of RBCs from different blood donors treated with a range of rEBA175-RII concentrations, and treated with neuraminidase (Neu). Each circle represents data from a single cell, solid line represents the median. Mean square amplitude ($h\ (q_x)^2\ (m)^2$) of contour fluctuation modes versus wave vector ($q_x$) of representative RBCs are shown in SI Figure S3. P-values comparing the treatment versus control, calculated using Mann-Whitney test (ns: non-significant, ** p<0.05, ** p<0.01, *** p<0.001, **** p<0.0001).*

**Figure 4.** rEBA175-RII mediated increase in tension is dependent on the GPA cytoplasmic tail. (A-B) summary of tension and bending modulus changes in MiV cells following rEBA175-RII incubation. Each circle represents data from a single cell, solid line represents the median. Mean square amplitude ($h\ (q_x)^2\ (m)^2$) of contour fluctuation modes versus wave vector ($q_x$) of

representative RBCs are shown in SI Figure S4. (C) Parasite invasion into MiV cells was measured by flow cytometry. Parasites used were a *P. falciparum* strain that invades using GPA (W2mefΔRh4) and a strain invading independently of this receptor (W2mefΔEBA175). P-values comparing the treatment versus control were calculated using the student's t-test (ns: non-significant, * *p<0.05, ** p<0.01, *** p<0.001, **** p<0.0001).*

**Figure 5.** RBCs treated with 7-KC to decrease bending modulus are more readily invaded than control RBCs. (A-B) RBCs pre-treated with Fluo-4AM (A) were incubated with rEBA175-RII and then stained with annexin V (B). Calcium influx (A) and phosphatidylserine exposure (B) were assessed by flow cytometry. (C-D) RBCs were treated with varying concentrations of 7-KC for 30 minutes, then washed and re-suspended in fresh media, before parasite schizonts were added. Parasite invasion (Relative Parasitemia %) was quantified by flow cytometry. Strains used were w2mefΔEBA175 (C) and w2mefΔRh4 (D). P-values comparing the treatment versus control were calculated using the student's t-test (ns: non-significant, * *p<0.05, ** p<0.01, *** p<0.001, **** p<0.0001).*

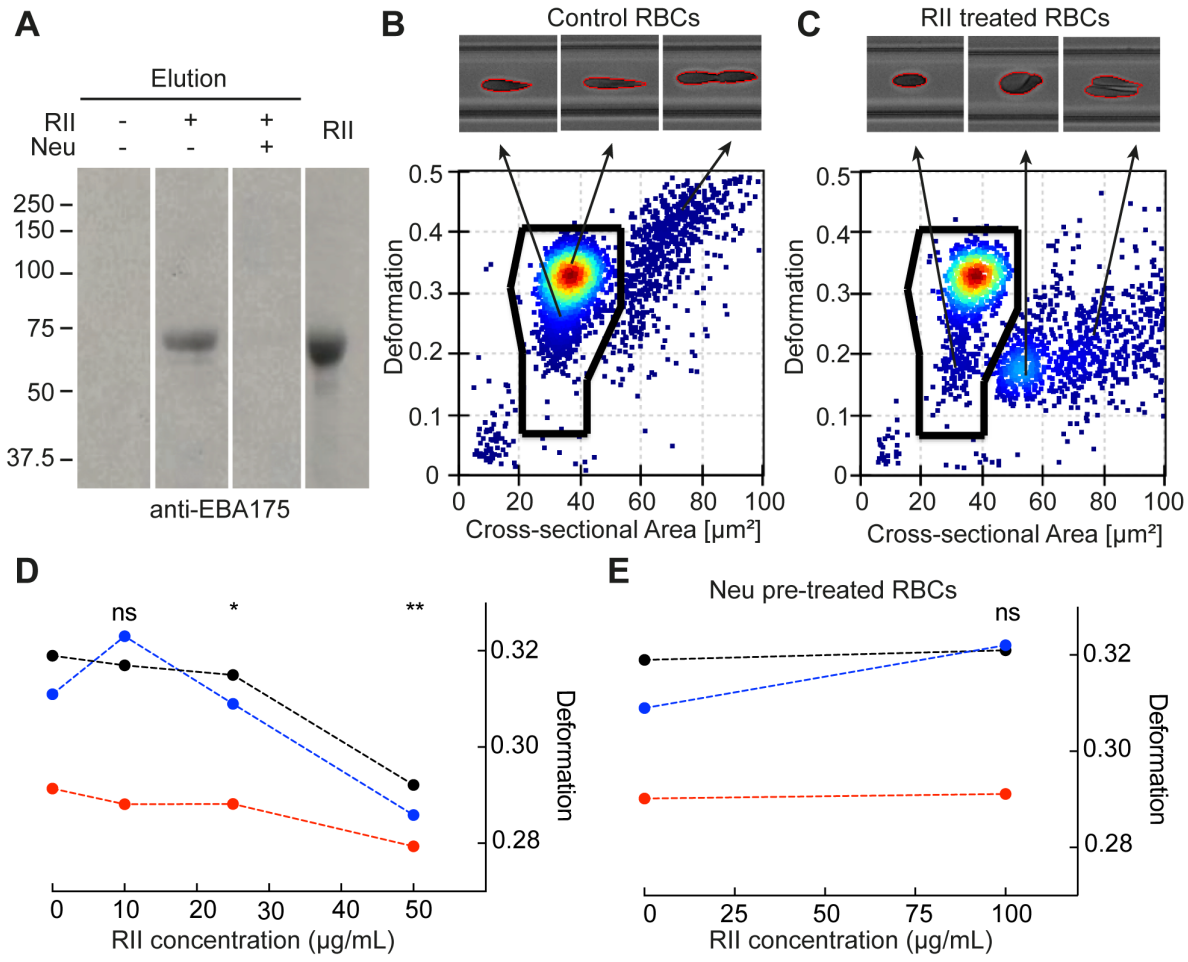
A
Elution
RII
Neu
RII
250
150
100
75
50
37.5
anti-EBA175
B
Control RBCs
Deformation
Cross-sectional Area [µm²]
C
RII treated RBCs
Deformation
Cross-sectional Area [µm²]
D
ns
*
**
Deformation
RII concentration (µg/mL)
E
Neu pre-treated RBCs
ns
Deformation
RII concentration (µg/mL)

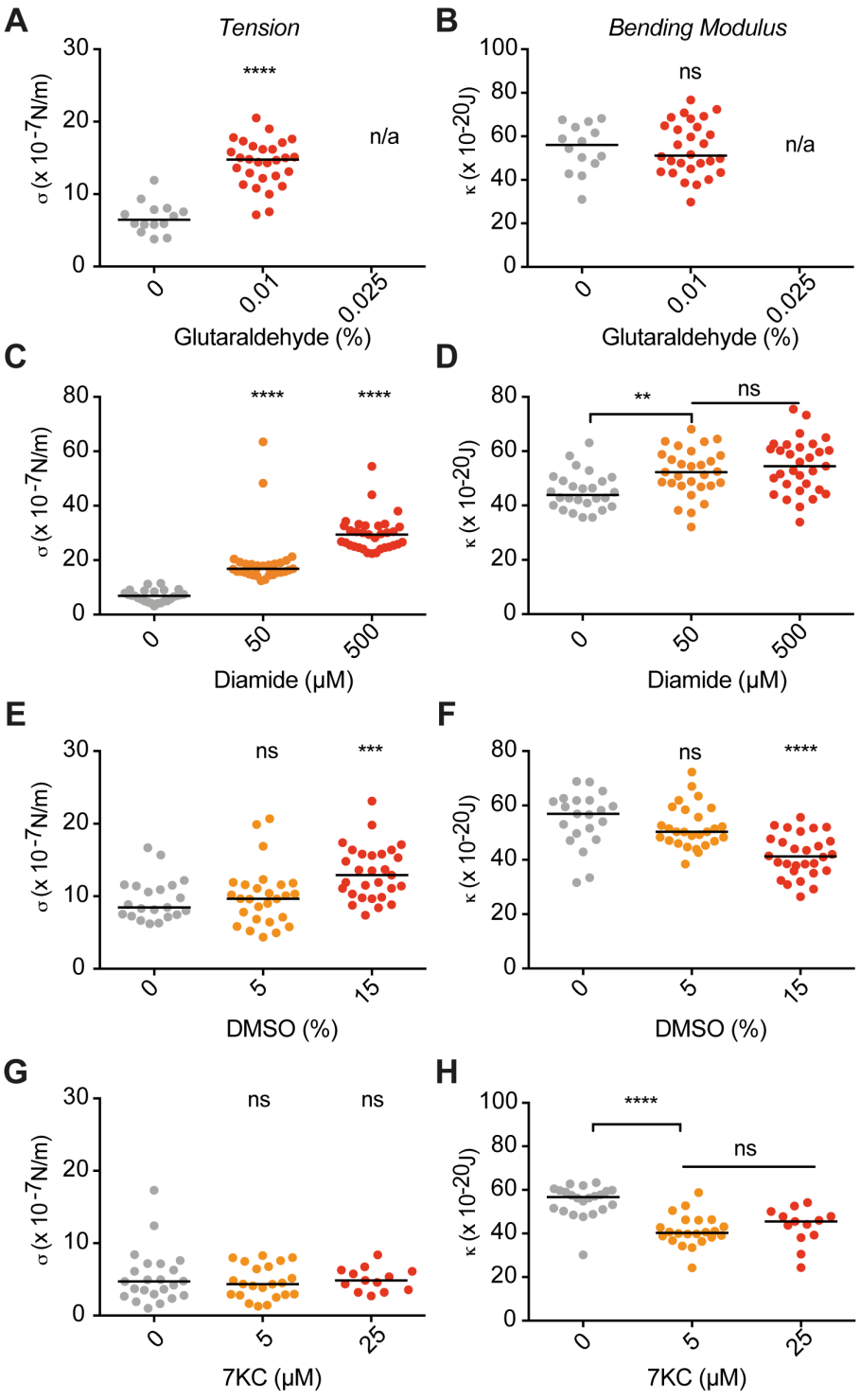
A
Tension
σ (x 10-7N/m)
****
n/a
Glutaraldehyde (%)
B
Bending Modulus
κ (x 10-20J)
ns
n/a
Glutaraldehyde (%)
C
****
****
Diamide (μM)
D
**
ns
Diamide (μM)
E
ns
***
DMSO (%)
F
ns
****
DMSO (%)
G
ns
ns
7KC (μM)
H
****
ns
7KC (μM)

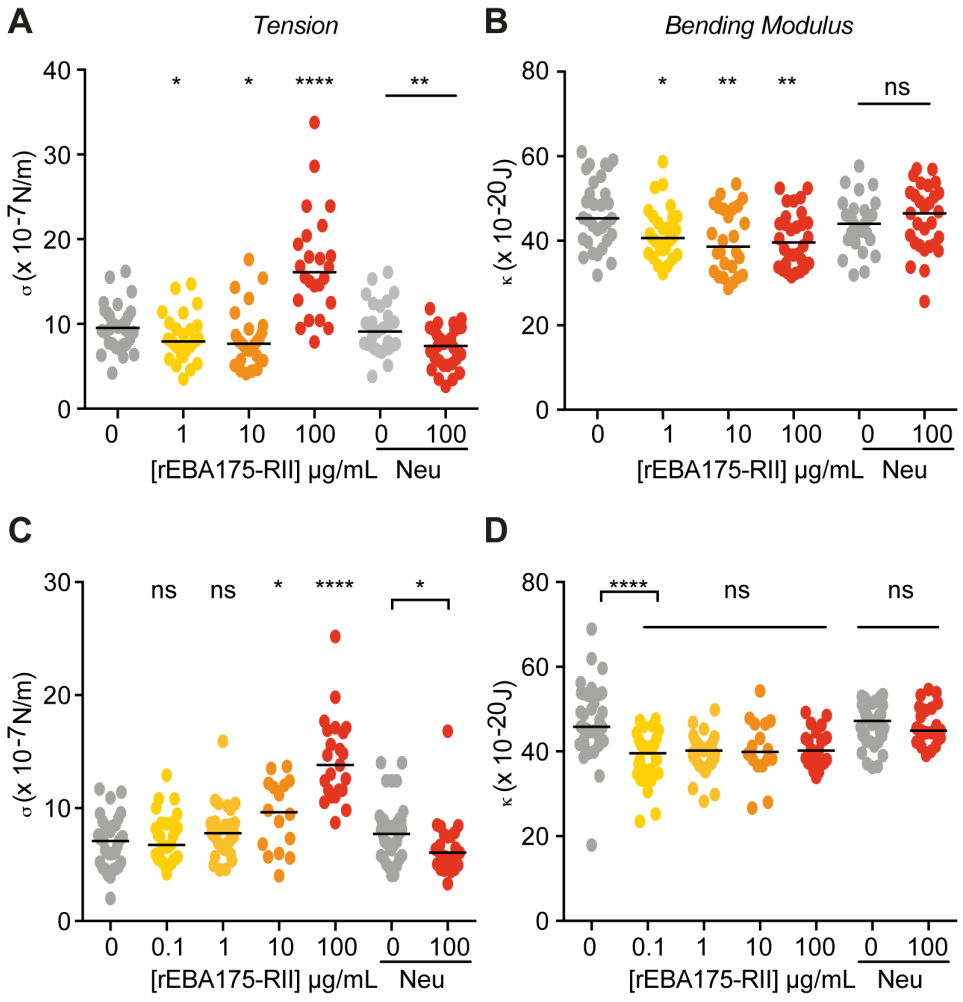
A
Tension
σ (x 10-7N/m)
40
30
20
10
0
*
*
****
**
0
1
10
100
0
100
[rEBA175-RII] µg/mL
Neu
B
Bending Modulus
κ (x 10-20J)
80
60
40
20
0
*
**
**
ns
0
1
10
100
0
100
[rEBA175-RII] µg/mL
Neu
C
σ (x 10-7N/m)
30
20
10
0
ns
ns
*
****
*
0
0.1
1
10
100
0
100
[rEBA175-RII] µg/mL
Neu
D
κ (x 10-20J)
80
60
40
20
0
****
ns
ns
0
0.1
1
10
100
0
100
[rEBA175-RII] µg/mL
Neu

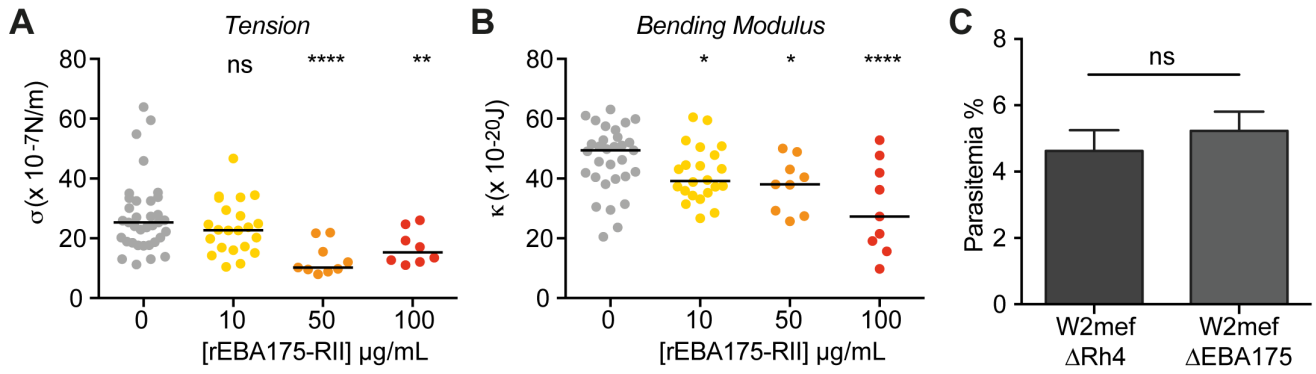
A
Tension
ns
****
**
σ(x 10-7N/m)
80
60
40
20
0
0
10
50
100
[rEBA175-RII] µg/mL
B
Bending Modulus
*
*
****
κ(x 10-20J)
80
60
40
20
0
0
10
50
100
[rEBA175-RII] µg/mL
C
ns
Parasitemia %
8
6
4
2
0
W2mef
ΔRh4
W2mef
ΔEBA175

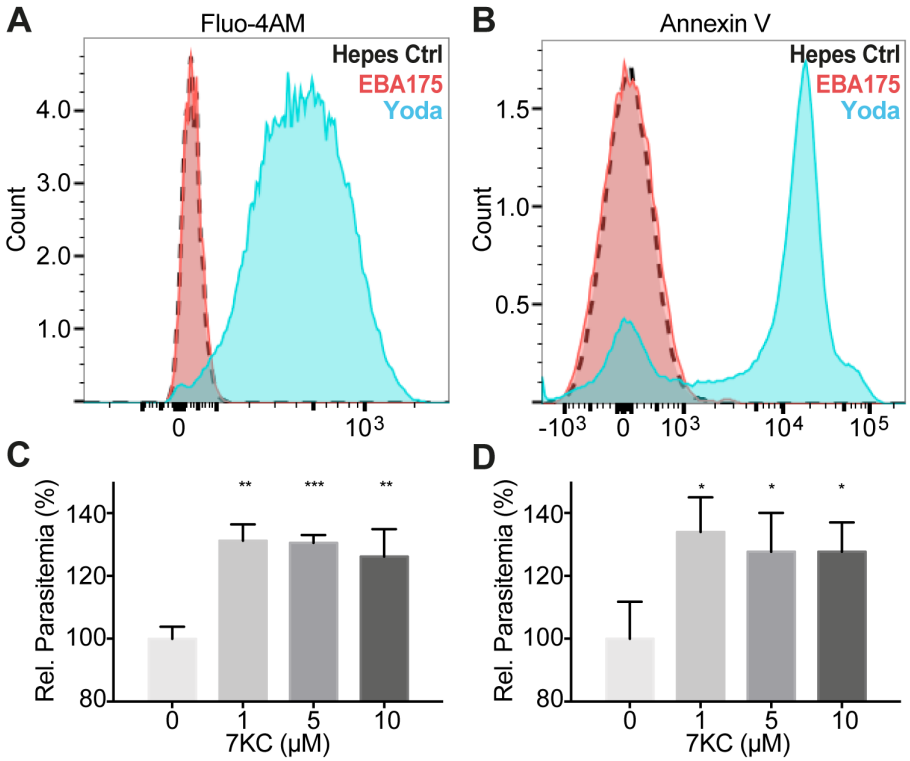
A
Fluo-4AM
Hepes Ctrl
EBA175
Yoda
Count
4.0
3.0
2.0
1.0
0
10^3
B
Annexin V
Hepes Ctrl
EBA175
Yoda
Count
1.5
1.0
0.5
-10^3
0
10^3
10^4
10^5
C
Rel. Parasitemia (%)
140
120
100
80
**
***
**
0
1
5
10
7KC (μM)
D
Rel. Parasitemia (%)
140
120
100
80
*
*
*
0
1
5
10
7KC (μM)

**SUPPORTING INFORMATION (SI) APPENDIX**

## SI Materials and Methods

### Parasite culturing

*P. falciparum* parasites (strains W2mefΔRh4, W2mefΔEBA175) were maintained in standard culture conditions (1) in human O+ erythrocytes at 4% hematocrit in complete RPMI-1640 media (Life Technologies) and synchronised using 5% sorbitol (Sigma-Aldrich) (2). RBCs were provided by the blood bank with Miltenberger V cells generously provided by Nicole Thornton (IBGRL). Frozen Miltenberger V cells were thawed in 37°C Alsever's solution (Sigma-Aldrich), centrifuged at 500g and the supernatant removed. Cells were then washed in PBS and stored at 4°C in Alsever's solution.

### Invasion & Growth assays

Schizont parasites were magnetically purified using a commercially available MACS system (Miltenyi Biotec) as previously described (3). Schizonts were added directly to fresh RBCs. For invasion experiments with 7-ketocholesterol (Sigma-Aldrich), RBCs were incubated with 7-ketocholesterol (1, 5, 10 μM) or equivalent DMSO control (0.2% final volume) for 45 minutes at 37ºC before being re-suspended into fresh media. After 16h, cells were washed in PBS, stained with SybrGreen (Sigma-Aldrich; 1:2,000 in PBS) for 20 minutes at room temperature protected from light, and washed before invasion was quantified by flow cytometry. 100,000 cells were acquired per well using FITC channel of the BD Fortessa flow cytometer. GFP fluorescence was plotted against forward-scatter and a gate was drawn for GFP-positive cells. Uninfected RBCs were used as a gating control.

### Erythrocyte binding assay and Western Blotting

Binding assays were performed as described (4) with eluate analysed for the presence of rEBA175-RII by western blotting using standard methods. Primary antibody used was mouse anti-EBA-175 (5) antibody [1:1,000] and secondary antibody was anti-mouse-HRP

[1:5000]. The blots were developed using ECL (Amersham).

**Annexin V and Fluo-4AM assay**

RBCs were washed in complete RPMI media and stained with Fluo-4AM (3 μM) for 30 minutes in the dark at 37° C. Cells were washed, incubated with 1 μg/ml rEBA175-RII, an equivalent volume of buffer (10 mM HEPES, pH 7.4, 150 mM NaCl), or 10 μM Yoda1 for 30 minutes at room temperature. RBCs were resuspended into 10 mM HEPES, pH 7.4; 140 mM NaCl, 2.5 mM $CaCl_2$ with 1% Annexin V for 10 minutes, then transferred into fresh binding buffer and analysed by flow cytometry. 100,000 cells were acquired per well using the FITC channel of the BD Fortessa Flow cytometer (Fluo-4AM) and the Cy-5 channel (Annexin-V).

**Statistical Analysis**

RT-DC data was analysed using a linear mixed effects model in R (6). Using package *lme4* (7) models were defined. Model M1 allows varying mean level and effect ('Random intercept and random slope model') while model M2 ('Null hypothesis') assumes no effect. Model M1 and M2 are then compared using a likelihood ratio test (8) and Wilks (9) theorem allows calculation of the p-value for the effect, with $p<0.05$ considered statistically significant.

GraphPad Prism (GraphPad Software Inc, USA) was used for analysing the statistical significance of flicker spectroscopy experiments and *P. falciparum* RBC invasion data. Prior to statistical analysis distribution of flicker spectroscopy data was assessed for normality, since the data was not normally distributed across all experiments, analysis was carried out using the Mann-Whitney test. Analysis was kept consistent across all flicker spectroscopy experiments. *P. falciparum* RBC invasion data was analysed using the student's t-test (unpaired, two-tailed), with $p < 0.05$ considered statistically significant.

**SI Figures**

**Figure S1**. Extracting the RBC tension and bending modulus from microscopy data. (A) The RBC contour (shape) is first determined in each video frame by radially integrating the image intensity (scale bar 5 μm) (B) the contour is then Fourier transformed to break down the contour shape into individual fluctuation modes and their associated amplitudes (modes 2 to 5 shown), (C) the fluctuation mode amplitudes are fitted to double parameter model to extract the tension (σ) and bending modulus (κ) (gray line). The coloured lines show the effect of multiplying (darker colours) or dividing (lighter colours) the tension (yellow lines) or bending modulus (blue lines) by a factor of 1.5. The effect of changes in the cell tension is most significant in the lower modes of the fluctuation power spectrum and the bending modulus has a larger influence on the amplitude of the higher modes. For full details see Yoon et. al (10).

**Figure S2.** Chemically-induced tension and bending modulus changes in RBCs measured by flicker spectroscopy. Summary of tension (σ) and bending modulus (κ) values for RBC treatments is shown in Figure 2. Here, mean square amplitude ($h\ (q_x)^2\ (m)^2$) of contour fluctuation modes versus wave vector ($q_x$) of representative RBCs is shown for Glutaraldehyde, (A), Diamide, (B), DMSO (C) and 7-KC (D). The solid line corresponds to the fit of the data using the equation described in Materials & Methods, the circles represent RBC contour fluctuation amplitudes of individual modes; only modes that are analysed (modes 5-20) are shown.

**Figure S3.** rEBA175-RII mediated tension and bending modulus changes measured by flicker spectroscopy. Summary of tension (σ) and bending modulus (κ) values of RBCs from different blood donors treated with a range of rEBA175-RII concentrations, and treated with neuraminidase (Neu) are shown in Figure 3. Here, mean square amplitude ($h\ (q_x)^2\ (m)^2$) of contour fluctuation modes versus wave vector ($q_x$) of representative RBCs is shown for two different donors (A-B). The solid line corresponds to the fit of the data using the equation described in Materials & Methods, the circles represent RBC contour fluctuation amplitudes of individual modes; modes 5-20 are shown.

**Figure S4.** rEBA175-RII mediated increase in tension is dependent on the GPA cytoplasmic tail. A summary of tension and bending modulus changes in MiV cells following rEBA175-RII incubation is shown in Figure 4. Here, mean square amplitude ($h\ (q_x)^2\ (m)^2$) of contour fluctuation modes versus wave vector ($q_x$) of representative RBCs are shown. Solid lines correspond to the fit of the data using the equation described in Materials & Methods, the circles represent RBC contour fluctuation amplitudes of individual modes; modes 5-20 are shown.

**Figure S5.** A model of EBA-175 mediated cytoskeletal and membrane changes during *P. falciparum* merozoite invasion of the red blood cell. (A) Prior to attachment, a proportion of GPA molecules are associated with the spectrin cytoskeleton, whilst others are free within the membrane. (B) GPA binding causes an increase in tension due to more extensive cytoskeletal cross-linking and a decrease in the RBC bending modulus, i.e. a reduction in the force requirement to achieve membrane bending/curvature.

**SI References**


1. Trager W & Jensen JB (1976) Human malaria parasites in continuous culture. *Science* 193(4254):673-675.
2. Lambros C & Vanderberg JP (1979) Synchronization of Plasmodium falciparum erythrocytic stages in culture. *J Parasitol* 65(3):418-420.
3. Boyle MJ*, et al.* (2010) Isolation of viable Plasmodium falciparum merozoites to define erythrocyte invasion events and advance vaccine and drug development. *Proc Natl Acad Sci USA* 107(32):14378-14383.
4. Baum J*, et al.* (2009) Reticulocyte-binding protein homologue 5 - An essential adhesin involved in invasion of human erythrocytes by Plasmodium falciparum. *Int J Parasitol* 39(3):371-380.
5. Triglia T*, et al.* (2011) Plasmodium falciparum merozoite invasion is inhibited by antibodies that target the PfRh2a and b binding domains. *PLoS Pathog* 7(6):e1002075.
6. R-Core-Team (2014) *R: A Language and Environment for Statistical Computing.* (R Foundation for Statistical Computing., Vienna, Austria).
7. Bates D, Maechler M, Bolker B, & Walker S (2015) Fitting Linear Mixed-Effects Models Using lme4. *J Statistical Software* 67:1-48.
8. Mood AM & Graybill FA (1963) *Introduction to the Theory of Statistics* (McGraw-Hill Book Company, Inc.) 2nd Edition Ed.
9. Wilks S (1938) The Large-Sample Distribution of the Likelihood Ratio for Testing Composite Hypotheses. *Annals of Mathematical Statistics* 9:60-62.
10. Yoon YZ*, et al.* (2009) Flickering analysis of erythrocyte mechanical properties: dependence on oxygenation level, cell shape, and hydration level. *Biophys J* 97(6):1606-1615.

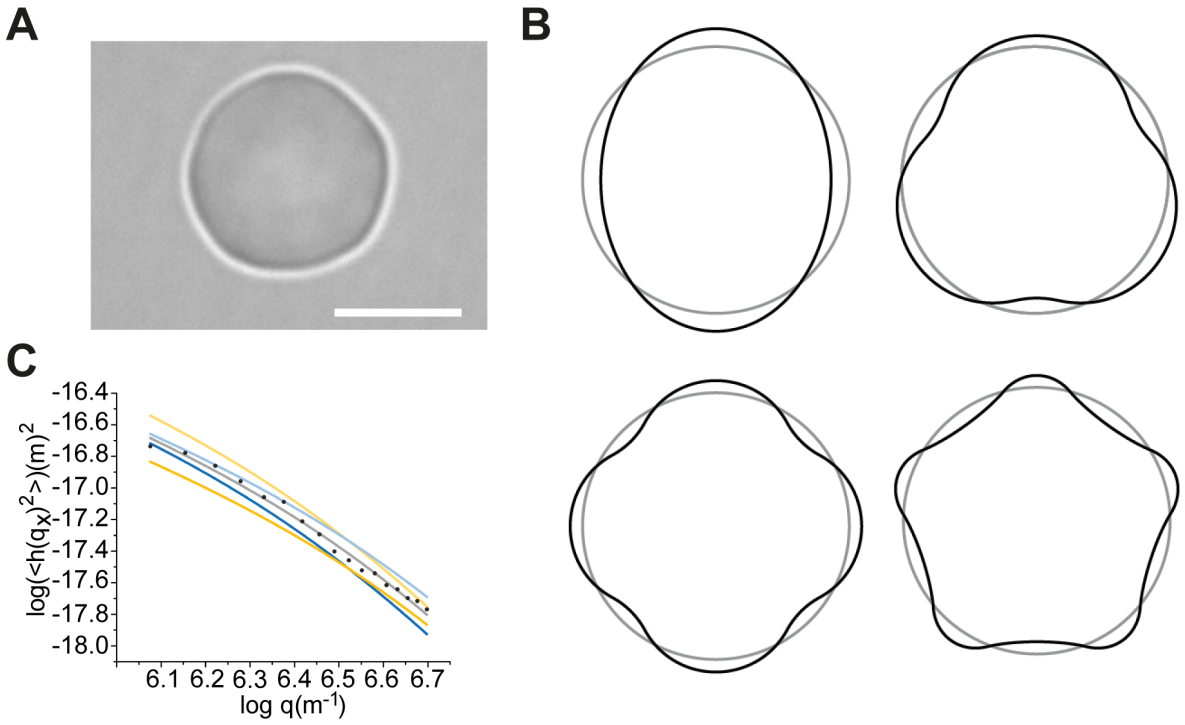
A
B
C
-16.4
-16.6
-16.8
-17.0
-17.2
-17.4
-17.6
-17.8
-18.0
log(<h(qx)2>)(m)2
6.1 6.2 6.3 6.4 6.5 6.6 6.7
log q(m-1)

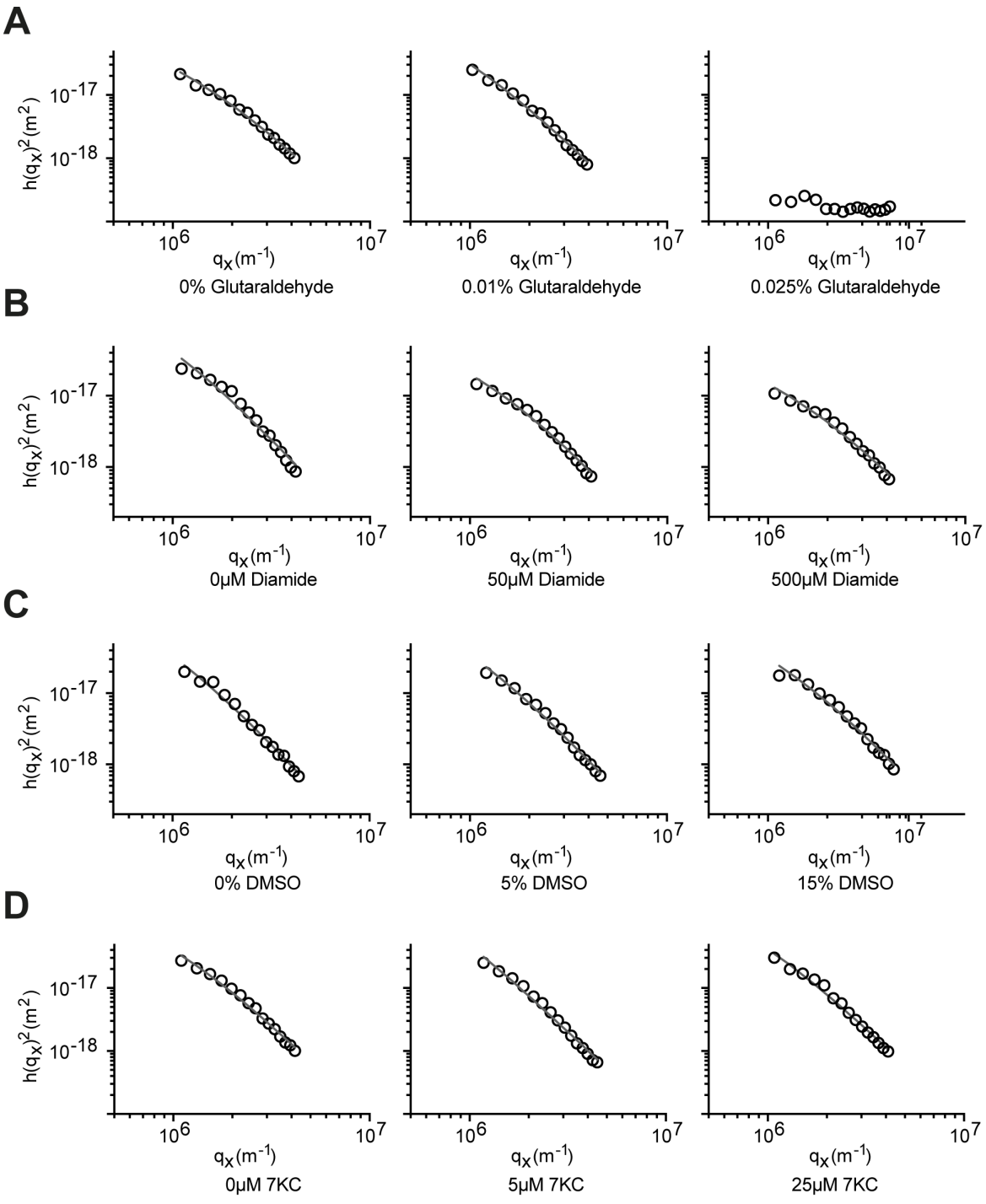
A
B
C
D
$h(q_x)^2(m^2)$
$10^{-17}$
$10^{-18}$
$10^6$
$10^7$
$q_x(m^{-1})$
0% Glutaraldehyde
0.01% Glutaraldehyde
0.025% Glutaraldehyde
0μM Diamide
50μM Diamide
500μM Diamide
0% DMSO
5% DMSO
15% DMSO
0μM 7KC
5μM 7KC
25μM 7KC

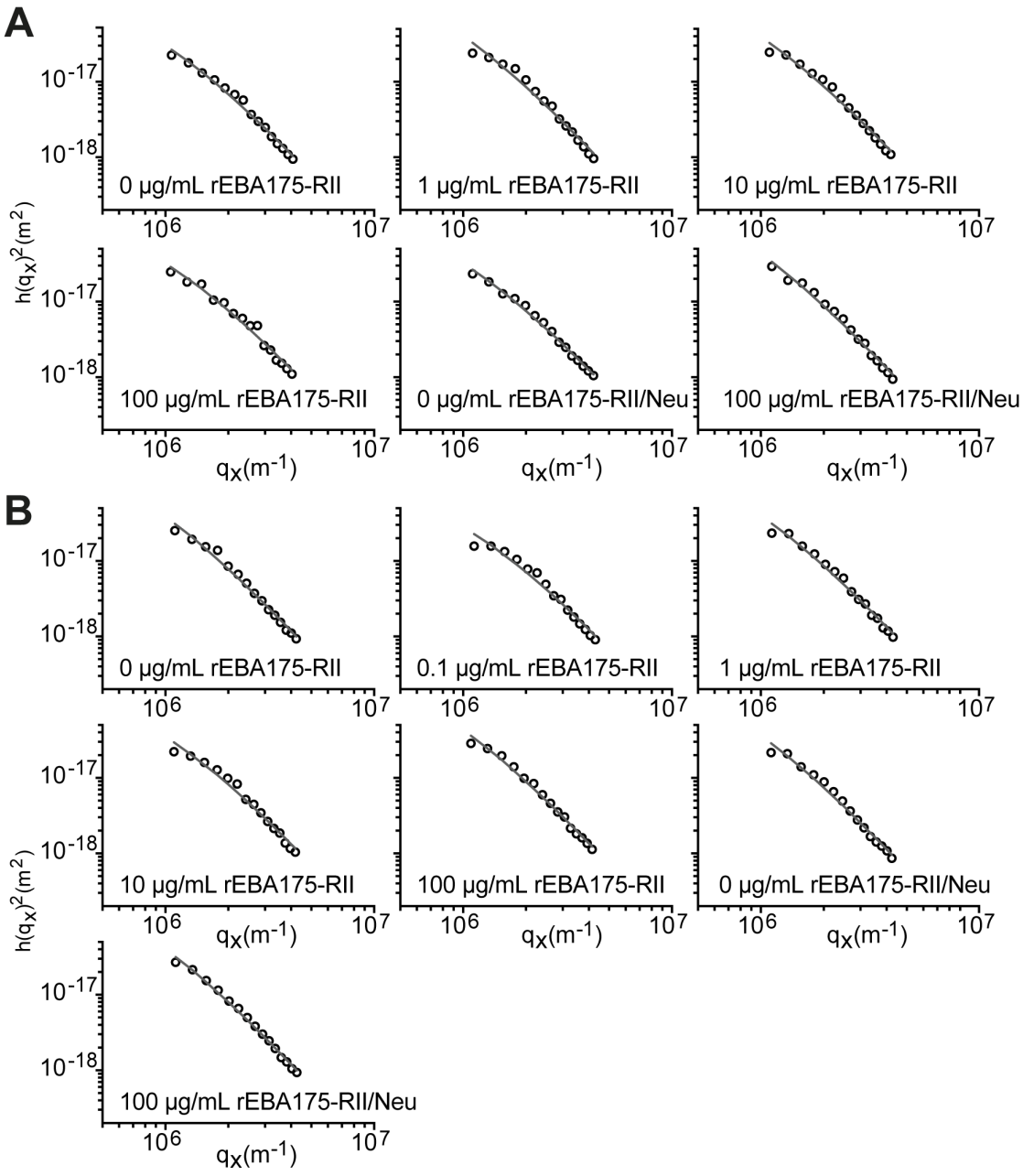
A
B
0 µg/mL rEBA175-RII
1 µg/mL rEBA175-RII
10 µg/mL rEBA175-RII
100 µg/mL rEBA175-RII
0 µg/mL rEBA175-RII/Neu
100 µg/mL rEBA175-RII/Neu
0.1 µg/mL rEBA175-RII
h(qx)2(m2)
qx(m-1)
10-17
10-18
106
107

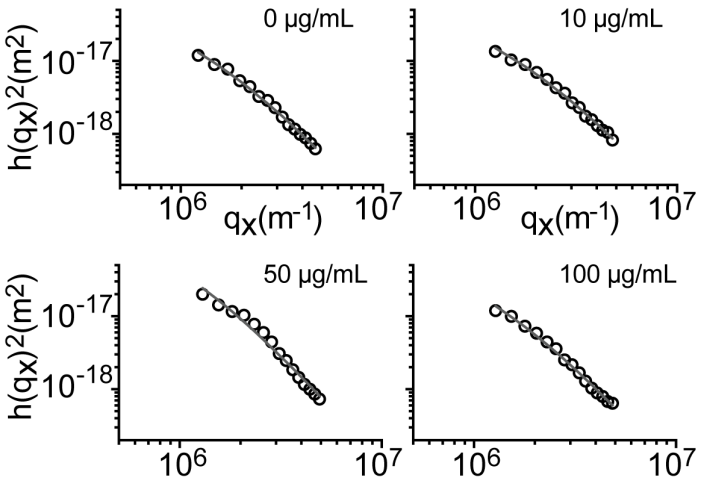
0 µg/mL
10 µg/mL
50 µg/mL
100 µg/mL
h(qx)2(m2)
10-17
10-18
10^6
10^7
qx(m-1)

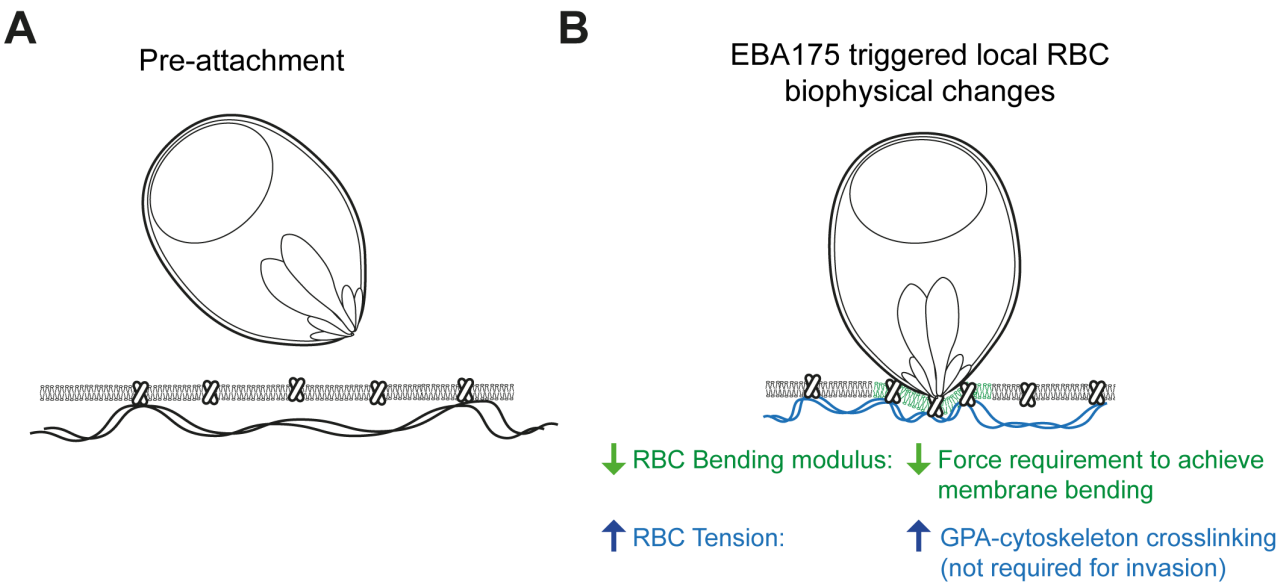
A
Pre-attachment
B
EBA175 triggered local RBC biophysical changes
RBC Bending modulus:
Force requirement to achieve membrane bending
RBC Tension:
GPA-cytoskeleton crosslinking (not required for invasion)